THE JOURNAL OF BIOLOGICAL CHEMISTRY VOL. 288, NO. 46, pp. 33376–33386, November 15, 2013

Thioesterase Superfamily Member 2/Acyl-CoA Thioesterase 13 (Them2/Acot13) Regulates Adaptive Thermogenesis in Mice*

Received for publication, May 2, 2013, and in revised form, September 17, 2013 Published, JBC Papers in Press, September 26, 2013, DOI 10.1074/jbc.M113.481408

Hye Won Kang[‡1,2], **Cafer Ozdemir**[‡1], **Yuki Kawano**[‡], **Katherine B. LeClair**[‡], **Cecile Vernochet**[§], **C. Ronald Kahn**[§], **Susan J. Hagen**[¶], **and David E. Cohen**[‡3]

From the [‡]*Department of Medicine, Division of Gastroenterology, Brigham and Women's Hospital, Harvard Medical School, Boston, Massachusetts 02115, the* [§]*Joslin Diabetes Center, Harvard Medical School, Boston, Massachusetts 02215, and the* [¶]*Department of Surgery, Beth Israel Deaconess Medical Center, Harvard Medical School, Boston, Massachusetts 02215*

Background: Thioesterase superfamily member 2 (Them2) is a long chain fatty acyl-CoA thioesterase that is enriched in brown adipose tissue (BAT).
Results: *Them2*$^{-/-}$ mice exhibit enhanced adaptive thermogenesis and increased fatty acid oxidation in BAT.
Conclusion: Them2 suppresses adaptive increases in energy expenditure by reducing BAT activity.
Significance: Them2 could represent an attractive target in the management of obesity.

Members of the acyl-CoA thioesterase (Acot) gene family hydrolyze fatty acyl-CoAs, but their biological functions remain incompletely understood. Thioesterase superfamily member 2 (Them2; synonym Acot13) is enriched in oxidative tissues, associated with mitochondria, and relatively specific for long chain fatty acyl-CoA substrates. Using *Them2*$^{-/-}$ mice, we have demonstrated key roles for Them2 in regulating hepatic glucose and lipid metabolism. However, reduced body weights and decreased adiposity in *Them2*$^{-/-}$ mice observed despite increased food consumption were not well explained. To explore a role in thermogenesis, mice were exposed to ambient temperatures ranging from thermoneutrality (30 °C) to cold (4 °C). In response to short term (24-h) exposures to decreasing ambient temperatures, *Them2*$^{-/-}$ mice exhibited increased adaptive responses in physical activity, food consumption, and energy expenditure when compared with *Them2*$^{+/+}$ mice. By contrast, genotype-dependent differences were not observed in mice that were equilibrated (96 h) at each ambient temperature. In brown adipose tissue, the absence of Them2 was associated with reduced lipid droplets, alterations in the ultrastructure of mitochondria, and increased expression of thermogenic genes. Indicative of a direct regulatory role for Them2 in heat production, cultured primary brown adipocytes from *Them2*$^{-/-}$ mice exhibited increased norepinephrine-mediated triglyceride hydrolysis and increased rates of O_2 consumption, together with elevated expression of thermogenic genes. At least in part by regulating intracellular fatty acid channeling, Them2 functions in brown adipose tissue to suppress adaptive increases in energy expenditure.

The hydrolysis of intracellular triglycerides and oxidation of fatty acids are essential to non-shivering thermogenesis mediated by brown adipose tissue (BAT).[4] In BAT of cold-exposed mice, free fatty acids are released by the action of hormone sensitive lipase in response to norepinephrine signaling, converted to fatty acyl-CoAs, and directed toward mitochondrial β-oxidation by long chain acyl-CoA synthetase (ACSL) 1 (1). Acyl-CoA thioesterases (Acots) are enzymes that catalyze the reverse reaction: hydrolysis of fatty acyl-CoA molecules into free fatty acids plus CoASH. Two distinct types of protein structure lead to similar enzymatic activities of 14 different Acots (2, 3). Type 1 enzymes (Acots 1–6) contain N-terminal β-sandwich and C-terminal α/β hydrolase domains and exhibit considerable amino acid sequence identity, whereas Type 2 enzymes (Acots 7–13, 15) utilize N-terminal hotdog fold thioesterase domains and are related principally by structure rather than sequence (2, 3). Four genes that were originally categorized as thioesterase superfamily members (*Them*) *1*, *2*, *4*, and *5*, (corresponding to *Acot 11*, *13*, *14*, and *15*, respectively) each appear to function in nutrient metabolism and energy homeostasis (4). Them1, which is enriched in BAT and markedly induced by cold ambient temperatures, functions to reduce energy expenditure (5). This supports the concept that the balance between synthesis and hydrolysis of fatty acyl-CoAs in BAT is important in the regulation of thermogenesis (6, 7).

We initially identified Them2 (synonym: Acot13) as an interacting partner for phosphatidylcholine transfer protein (PC-TP, synonym: StarD2 (steroidogenic acute regulatory protein-related lipid transfer domain 2)) (8), which is a highly spe-

* This work was supported, in whole or in part, by National Institutes of Health Grants R01 DK056626 and R37 DK048873 (to D. E. C.), R01 DK082659 (to C. R. K.), and the Harvard Digestive Diseases Center (Grant P30 DK034854).
[1] Both authors contributed equally to this work.
[2] The recipient of a Founders Affiliate Postdoctoral Fellowship from the American Heart Association.
[3] To whom correspondence should be addressed: Brigham and Women's Hospital, 77 Avenue Louis Pasteur, HIM 941, Boston, MA 02115. Tel.: 617-525-5090; Fax: 617-525-5100; E-mail: dcohen@partners.org.

[4] The abbreviations used are: BAT, brown adipose tissue; Acot, acyl-CoA thioesterase; CLAMS, Comprehensive Laboratory Animal Monitoring System; FCCP, carbonyl cyanide-*p*-trifluoromethoxyphenylhydrazone; microCT, micro-computed tomography; OCR, O_2 consumption rate; PC-TP, phosphatidylcholine transfer protein; PGC1α, peroxisome proliferator-activated receptor-γ coactivator 1α; PPARα, peroxisome proliferator-activated receptor α; RER, respiratory exchange ratio(s); Them, thioesterase superfamily member; UCP1, uncoupling protein 1; VCO_2, rate of CO_2 production; VO_2, rate of O_2 consumption.

cific intracellular lipid-binding protein. Them2 is enriched in liver and oxidative tissues, including BAT, and is primarily associated with mitochondria (9). Purified recombinant Them2 exhibits substrate specificity for long chain fatty acyl-CoAs *in vitro* (9, 10). To gain insights into the biological function of Them2, we created *Them2*$^{-/-}$ mice (11), which revealed key contributions to the regulation of fatty acid and glucose metabolism in the liver.

In this prior study, *Them2*$^{-/-}$ mice also exhibited reduced body weights and decreased adiposity despite increased food consumption (11). Notwithstanding a very modest reduction in lipid absorption, these changes were not well explained. The present study was designed to systematically explore a regulatory role for Them2 in energy homeostasis. As functions of decreasing ambient temperature from thermoneutrality (30 °C) to cold (4 °C), *Them2*$^{-/-}$ mice exhibited adaptive increases in energy expenditure that were not observed when mice were equilibrated for more prolonged periods at each temperature. Within BAT, the absence of Them2 led to decreased lipid droplet sizes, ultrastructural changes consistent with increased fatty acid uptake into mitochondria, and up-regulation of thermogenic genes. In cultured brown adipocytes from *Them2*$^{-/-}$ mice, more rapid norepinephrine-mediated hydrolysis of triglycerides and fatty acid oxidation was also accompanied by increased thermogenic gene expression. When taken together, these findings indicate a key role for Them2 in the control of adaptive thermogenesis.

EXPERIMENTAL PROCEDURES

Animals and Diets—Male 9–12-week-old *Them2*$^{-/-}$ and littermate *Them2*$^{+/+}$ mice were as described previously (11). Mice were housed in an animal barrier facility with a standard chow diet (PicoLab Rodent Diet 20, 5053, LabDiets, St. Louis, MO) with a 12-h light/dark cycle (light cycle, 6 a.m. to 6 p.m.; dark cycle, 6 p.m. to 6 a.m.) at 22 ± 1 °C. In experiments to measure core body temperature, mice were implanted with small intraperitoneal temperature transponders (Mini Mitter, Bend, OR). Briefly, mice were anesthetized using 1–2% isoflurane vapor, the abdomen was shaved and cleaned with betadine and alcohol, and the abdominal cavity was entered by way of a 2-cm midline abdominal skin incision positioned 1 cm below the diaphragm along the linea alba. The temperature transponder was positioned in the posterior aspect of abdominal cavity underneath the intestines and then sutured to the peritoneum. The abdominal cavity was then closed using an absorbable suture in a continuous interlocking running stitch. The skin was closed with monofilament non-reactive sutures using interrupted mattress stitches. Mice were kept on a warm water blanket (Gaymar Industries, Orchard Park, NY) during the surgery and recovery. Mice were returned to their cages and allowed to fully recover for 1 week prior to experiments. Upon completion of experiments, mice were euthanized using CO_2 to harvest BAT, which was snap-frozen in liquid N_2 and kept at −80 °C. Protocols for animal use and euthanasia were approved by the institutional committee of Harvard Medical School.

Core Body Temperature, Indirect Calorimetry, Physical Activity, and Food Consumption—Mice were transferred to individual metabolic cages without bedding, which were placed in a temperature-controlled Comprehensive Laboratory Animal Monitoring System (CLAMS: Columbus Instruments, Columbus, OH) with free access to diet and tap water in a 12-h light/dark cycle. Mice were subjected to non-invasive monitoring of gas exchange, physical activity, food intake, and core body temperature. Core body temperature and rates (ml/kg/h) of O_2 consumption (VO_2) and CO_2 production (VCO_2) were determined at 11-min intervals. Values were normalized to lean body mass, which was derived by multiplying total body weight by the percentage of lean body weight for mice housed at room temperature (~22 °C) as quantified *in situ* by micro-computed tomography (microCT) at the Longwood Small Animal Imaging Facility (Beth Israel Deaconess Medical Center) (11). Respiratory exchange ratios (RER) were calculated as the ratio of VCO_2 to VO_2. Rates of energy expenditure (kJ/h) were calculated from gas exchange (12). Cumulative values of energy expenditure (kJ) (13) were adjusted for differences in lean body weight and compared by analysis of covariance (14) using VassarStats.

Physical activity was determined according to beam breaks within a grid of photosensors built into the cages. Total activity was defined as the total number of beam breaks, whereas ambulatory activity was determined as successive beam breaks within the grid. Food consumption was determined by measuring the cumulative amount of food eaten using a balance connected to each cage in the CLAMS apparatus. For experiments designed to assess adaptive thermogenesis, mice were acclimated first at 30 °C for 24 h. The ambient temperature was then reduced every 24 h. Each mouse was weighed prior to being placed in the CLAMS and again immediately following its removal. Because preliminary analysis did not reveal appreciable differences in values of energy expenditure when adjusted to weights of mice before or after housing in the CLAMS, we used the initial weight for the data analysis at each temperature. To evaluate energy balance closer to steady state conditions, mice were equilibrated for 48 h at each temperature and then studied for 48 h prior to reducing the ambient temperature. In these experiments, each mouse was weighed at the beginning and end of exposure to each ambient temperature. The weight of the mice during the data recording period for each temperature was estimated by averaging the initial and final body weights at that temperature and then averaging this value with final body weight at the same temperature. In selected experiments designed to examine the effects of light cycle and access to food, mice were acclimated for 24 h at 22 °C and then studied at the same temperature. Because we could only measure body composition of mice at room temperature (~22 °C), calculations of lean body mass for the analysis of calorimetry data did not account for potential variations in body composition due to changes in ambient temperatures. The response of energy expenditure to changes in ambient temperature (kJ/°C) was quantified for individual mice by calculating the slope of the linear regression line, Δenergy expenditure/Δambient temperature.

BAT Mass, Histology, and Ultrastructure—BAT mass was quantified *in situ* by microCT as described above. Upon harvesting, BAT was stored in Bouin's fixative solution. Hematoxylin and eosin staining was performed by the Rodent Histopa-

thology Core Facility of the Dana-Farber/Harvard Cancer Center. Ultrastructural analysis was performed using electron microscopy as described previously (15). Briefly, freshly harvested BAT from 13-week-old mice was fixed, dehydrated, and embedded in LX112 resin (Ladd Research Industries, Burlington, VT). Ultrathin sections were cut using a Leica Ultracut E ultramicrotome (Leica Microsystems, Inc., Deerfield, IL) and then imaged with a JEOL 1400 electron microscope (JEOL USA, Inc., Peabody, MA). Images were taken with a Gatan CCD camera (Gatan, Warrendale, PA).

Fatty Acyl-CoA Concentrations, Rates of Fatty Acid Oxidation, and Acyl-CoA Thioesterase Activities in BAT—Long chain fatty acyl-CoA esters in BAT were analyzed by electrospray ionization-MS/MS in the Mouse Metabolic Phenotype Center at Yale University School of Medicine (New Haven, CT). Rates of fatty acid oxidation were measured in BAT homogenates as described previously using [1-^{14}C]palmitic acid (specific activity 55 mCi/mmol, American Radiolabeled Chemicals, St. Louis, MO) to determine the formation of acid-soluble metabolites (11). To measure fatty acyl-CoA thioesterase activity, BAT was homogenized and then centrifuged at 12,000 × *g* for 1 min. The top layer containing fat was removed. Enzyme activity was then determined in BAT homogenates, as well as isolated mitochondria as described previously (11). Briefly, enzymatic activity was determined by measuring the time-dependent reaction of 5,5′-dithiobis (nitrobenzoic acid) with CoASH that was cleaved from fatty acyl-CoAs. Reactions were initiated with 50 μg of protein in a 200-μl reaction buffer containing 50 mM KCl, 10 mM Hepes (pH 7.5), 0.3 mM 5,5′-dithiobis (nitrobenzoic acid), and myristoyl-CoA (Avanti Polar Lipids Inc., Alabaster, AL) as an exogenous substrate. Values of initial velocity (V_o) were determined from spectrophotometric readings, which were taken every min for 60 min at 412 nm and 37 °C using a SpectraMax M5 microplate reader (Molecular Devices, Sunnyvale, CA). Values of K_m and V_{max} were calculated according to the Michaelis-Menten equation (9).

Mitochondrial DNA and Citrate Synthase Activity in BAT—DNA was extracted from BAT using the DNeasy blood and tissue kit (Qiagen, Valencia, CA) according to the manufacturer's protocol. Ten ng of total DNA was used as template for PCR to determine the relative copy number of mitochondrial DNA normalized to β-globin DNA (16). Citrate synthase activity was measured in BAT as described previously (15).

Primary Culture and Differentiation of Brown Preadipocytes—Primary brown preadipocytes were isolated from interscapular BAT of 4–5-week-old mice (n = 8/group), cultured, and differentiated as described previously (15).

Rates of Lipolysis—Norepinephrine-induced lipolysis was measured in fully differentiated primary brown adipocytes by measuring glycerol released into culture media using a free glycerol determination kit (Sigma-Aldrich) as described (17). Briefly, fully differentiated primary brown adipocytes were incubated for 1 h in phenol red-free DMEM containing 2% fatty acid-free bovine serum albumin. The media were then replaced by the same media plus 1 μM L-(−)-norepinephrine-(+) bitartrate (Calbiochem). The media were then sampled periodically during a 3-h incubation period to determine glycerol concentrations. The data were normalized to cellular protein concentrations.

Cellular O_2 Consumption Rate (OCR)—Primary brown preadipocytes collected from BAT of mice were seeded at a density of 17,500 cells/cm^2 in customized Seahorse 24-well plates (Seahorse Bioscience, North Billerica, MA) and differentiated as described previously (15). Mature brown adipocytes were incubated in the absence of CO_2 for 1 h at 37 °C in unbuffered DMEM containing 25 mM glucose, 10 mM sodium pyruvate, but no sodium carbonate (pH 7.4). Plates were then loaded into an XF24 extracellular flux analyzer (Seahorse Bioscience) and exposed to either 1 μM norepinephrine or sequentially to 1 μM oligomycin, 0.5 μM carbonyl cyanide-*p*-trifluoromethoxyphenyl-hydrazone (FCCP), and 1 μM rotenone (16). OCR values were determined using eight replicates per genotype from O_2 concentrations measured for 2 min at 8-min intervals, which included a 3-min mixing period and a 3-min waiting period (16). OCR values are represented either as pmol/min/mg of protein or as the percentage of change when compared with basal OCR values.

Quantitative Real-time PCR—Total RNA was extracted from BAT or cultured brown adipocytes using TRIzol reagent, and cDNA was synthesized using a SuperScript III cDNA synthesis kit (both from Invitrogen). Measurements were performed using a Roche 480 LightCycler (Roche Applied Sciences). Ribosomal protein L32 (*RPL32*) was used as an invariant gene. To examine the influence of ambient temperature on gene expression, mice were housed at fixed ambient temperature for 24 h, after which interscapular BAT was immediately excised, snap-frozen in liquid N_2, and stored at −80 °C.

Statistics—Data are reported as mean ± S.E. Differences were evaluated using a two-tailed unpaired Student's t test (Prism 5, GraphPad Software Inc., La Jolla, CA). Differences were considered significant for $p < 0.05$.

RESULTS

Them2 Regulates the Adaptive Thermogenesis but Not Energy Balance near Steady State—Fig. 1 demonstrates the influence of Them2 expression on the adaptive response to ambient temperature of core body temperature, physical activity, and food consumption. When maintained at 30 °C, *Them2*$^{-/-}$ mice exhibited similar core body temperatures to *Them2*$^{+/+}$ mice during the light phase (Fig. 1*A*). There were slight elevations in the core body temperatures of *Them2*$^{-/-}$ mice in excess of those observed for *Them2*$^{+/+}$ mice early during the dark phase. This pattern became more pronounced at 22 °C because *Them2*$^{-/-}$ mice exhibited the same elevations in core body temperature as observed at 30 °C, whereas the core body temperature of *Them2*$^{+/+}$ mice decreased. At 4 °C, genotype-specific differences were eliminated and diurnal variations in core body temperatures were also lost.

Mean core body temperatures decreased linearly as functions of decreasing ambient temperatures, but did not differ significantly between genotypes (Fig. 1*B*) over the 24-h period or during the 12-h dark and light phases. Although food consumption was reduced during the light phase in *Them2*$^{-/-}$ mice at 30 °C, it was increased when compared with *Them2*$^{+/+}$ mice during the dark phase (Fig. 1*C*). When mice were housed

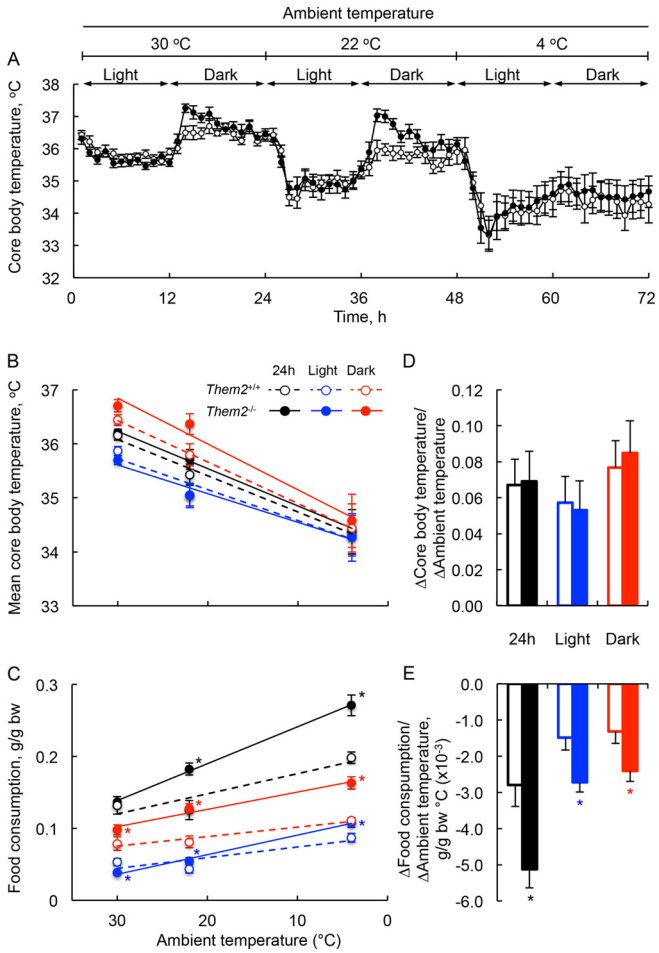

FIGURE 1. **Influence of Them2 expression on the adaptation of core body temperature and food consumption to changes ambient temperature.** Mice were housed individually in the CLAMS. After an initial 24-h equilibration period at 30 °C in the CLAMS, data were recorded for 24 h at each ambient temperature. CLAMS data were recorded for each mouse at 11-min intervals, but for clarity are presented as average hourly values in this and subsequent figures. *A*, core body temperatures were measured by transmitters implanted into the abdominal cavity ($n = 9$/group). *B* and *C*, linear dependence on ambient temperature of mean core body temperature (*B*) and food consumption ($n = 12$/group) (*C*) during the 24-h period, as well as the 12-h light and dark phases. *bw*, body weight. *D* and *E*, the responses of core body temperature (ΔCore body temperature/ΔAmbient temperature) (*D*) and food intake (ΔFood consumption/ΔAmbient temperature) (*E*) were determined by calculating slopes of linear regression lines for individual mice in *panels B* and *C*, respectively. *, $p < 0.05$, $Them2^{+/+}$ *versus* $Them2^{-/-}$.

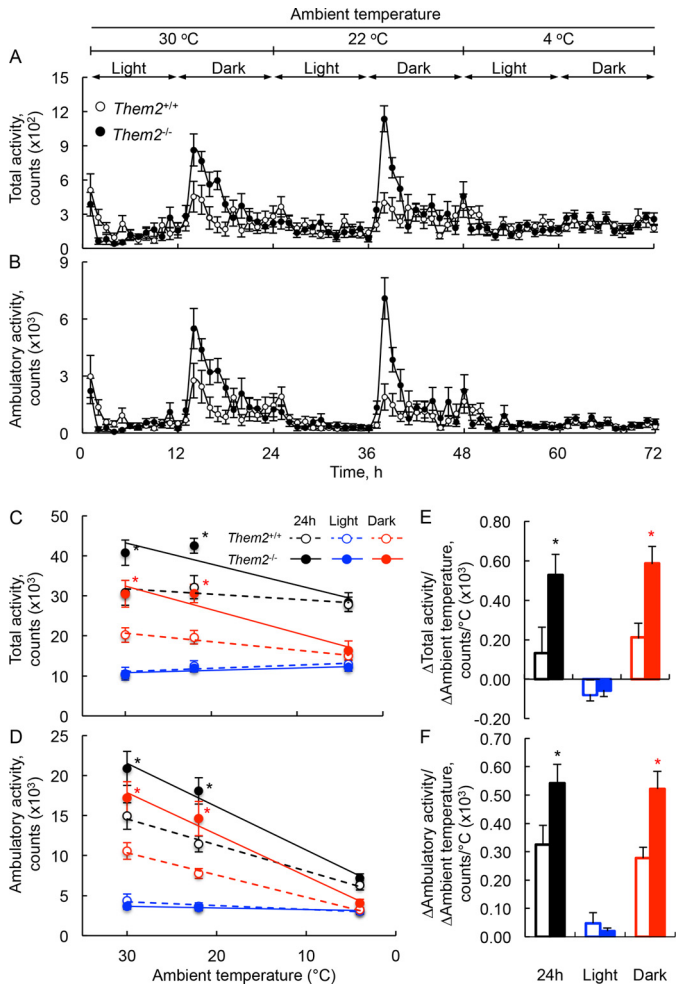

FIGURE 2. **Influence of Them2 expression on the adaptation of physical activity to ambient temperature.** *A* and *B*, total (*A*) and ambulatory (*B*) activities were monitored ($n = 12$/group) in the CLAMS experiment described in the legend for Fig. 1. *C* and *D*, total (*C*) and ambulatory (*D*) activities were determined for the 24-h period, as well as the 12-h light and dark phases indicated in *panels A* and *B*, respectively. *E* and *F*, the responses of total activity (ΔTotal activity/ΔAmbient temperature) (*E*) and ambulatory activity (ΔAmbulatory activity/ΔAmbient temperature) (*F*) activity were determined by calculating slopes of linear regression lines for individual mice in *panels C* and *D*, respectively. *, $p < 0.05$, $Them2^{+/+}$ *versus* $Them2^{-/-}$.

at 22 °C, $Them2^{-/-}$ mice consumed more food than $Them2^{+/+}$ mice. This increase was slight during the light phase. During the dark phase, food consumption increased for both genotypes, but was higher in $Them2^{-/-}$ when compared with $Them2^{+/+}$ mice. When the ambient temperature was reduced to 4 °C, food intake was greater in $Them2^{-/-}$ mice during both the light and the dark phases. Response to ambient temperature was calculated as the mean of slope values of linear regression lines for each mouse. Although the response of core body temperature did not differ between genotypes either over the 24-h period or during the dark and light phases (Fig. 1*D*), the response of food intake to ambient temperature was greater in $Them2^{-/-}$ mice during the 24-h period due to effects observed in both the light and the dark phases (Fig. 1*E*).

Fig. 2 shows the influence of ambient temperature on adaptive changes in mouse physical activities. Changes in total (Fig. 2*A*) and ambulatory (Fig. 2*B*) activity largely mirrored the changes in core body temperature. $Them2^{-/-}$ mice were more active over 24 h and during the dark phase at both 30 °C and 22 °C, as reflected by increased total (Fig. 2*C*) and ambulatory (Fig. 2*D*) activity. The responses of total (Fig. 2*E*) and ambulatory (Fig. 2*F*) activity were greater in $Them2^{-/-}$ mice for the 24-h period because of the effects of Them2 expression on the dark phase.

Consistent with prior observations (11), $Them2^{+/+}$ mice were initially heavier (g) than $Them2^{-/-}$ mice ($Them2^{+/+}$, 28.0 ± 0.6; $Them2^{-/-}$, 25.7 ± 0.5), but lost more weight over the course of the experiment, so that there were no differences in body weight after 24 h at 4 °C ($Them2^{+/+}$, 26.3 ± 0.7; $Them2^{-/-}$, 25.4 ± 0.5). At 22 °C, the percentage of lean body mass was higher in $Them2^{-/-}$ (97.3 ± 0.6) than $Them2^{+/+}$ (92.7 ± 0.4) mice.

Fig. 3 demonstrates the influence of Them2 expression on gas exchange under the same conditions. At 30 °C, $Them2^{+/+}$

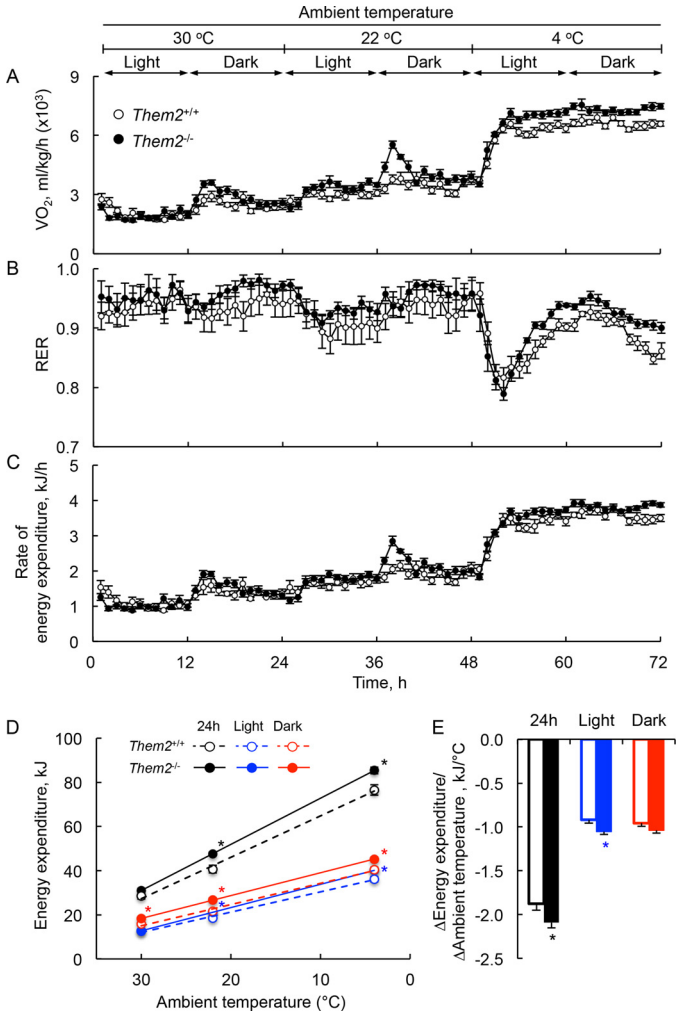

FIGURE 3. **Influence of Them2 expression on the adaptation of energy expenditure to ambient temperature.** *A–C*, VO_2 (*A*) and RER (*B*) were monitored ($n = 9$/group) in the CLAMS experiment described in the legend for Fig. 1 and used to calculate the rate of energy expenditure (*C*). *D*, cumulative values of energy expenditure for the 24-h period, as well as the 12-h light and dark phases indicated in *panel A*, were calculated and adjusted for lean body mass by analysis of covariance as described under "Experimental Procedures." *E*, the responses of energy expenditure (ΔEnergy expenditure/ ΔAmbient temperature) were determined by calculating slopes of linear regression lines for individual mice in *panel C*. *, $p < 0.05$, $Them2^{+/+}$ *versus* $Them2^{-/-}$.

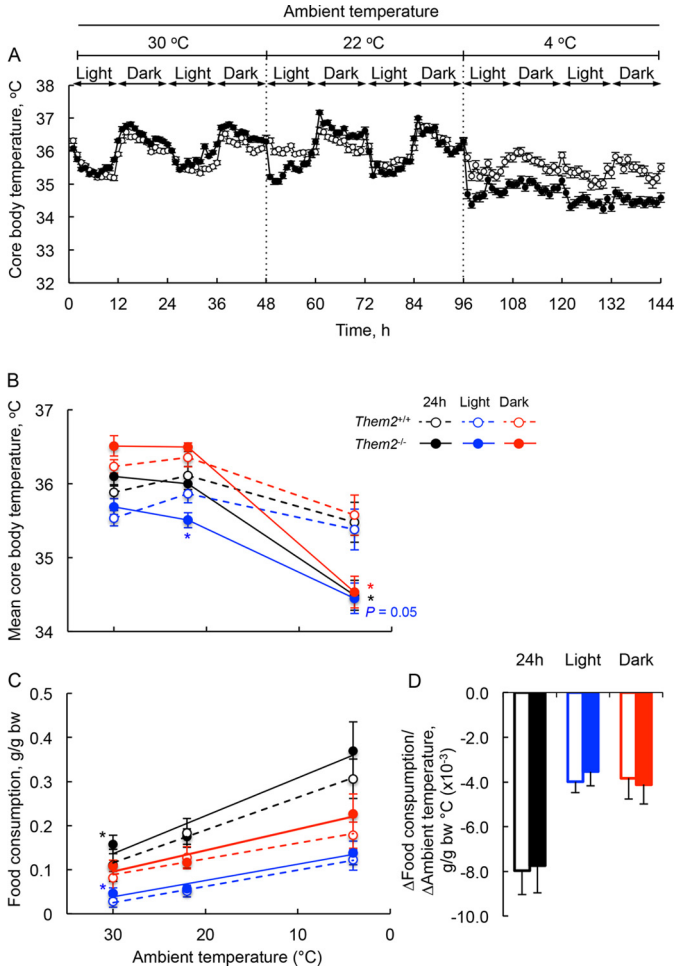

FIGURE 4. **Influence of Them2 expression on core body temperature and food consumption in ambient temperature-equilibrated mice.** *A* and *B*, core body temperatures ($Them2^{+/+}$, $n = 8$; $Them2^{-/-}$, $n = 9$) (*A*) and mean core body temperatures (*B*) were determined for the 48-h period, as well as the two 12-h light and dark phases indicated. *Vertical dashed lines* denote intervening 48-h equilibration periods. *C*, linear dependence of food consumption on ambient temperature ($n = 12$/group). *bw*, body weight. *D*, responses of food intake to changes in ambient temperature (ΔFood consumption/ΔAmbient temperature) were determined by calculating slopes of linear regression lines for individual mice in *panel B*. *, $p < 0.05$, $Them2^{+/+}$ *versus* $Them2^{-/-}$.

and $Them2^{-/-}$ mice exhibited similar values of VO_2 (Fig. 3*A*). At the beginning of the dark phase, VO_2 values increased slightly for both genotypes, but this increase was greater in $Them2^{-/-}$ mice. When the ambient temperature was reduced to 22 °C, VO_2 values increased during both the dark and the light phases. There was a transient increase observed at the beginning of dark phase, and this was again accentuated for $Them2^{-/-}$ mice. Upon reducing the ambient temperature to 4 °C, there was a sharp rise in VO_2 values for both genotypes, with $Them2^{-/-}$ mice exhibiting higher values of VO_2 during both the light and the dark phases. There were no significant differences in RER values between two genotypes at either 30 °C or 22 °C (Fig. 3*B*). Exposure to an ambient temperature of 4 °C resulted in a decline in RER values for both genotypes, which gradually increased during the light phase and then decreased during the dark phase. Following the initial period of adaptation to 4 °C, RER values for $Them2^{-/-}$ mice remained slightly higher than for $Them2^{+/+}$ mice. Rates of energy expenditure (Fig. 3*C*) largely paralleled VO_2 values (Fig. 3*A*). Cumulative values of energy expenditure were higher in $Them2^{-/-}$ mice over the 24-h period, as well as during both the light and the dark phases at 22 and 4 °C, but only during the dark phase at 30 °C (Fig. 3*D*). For both genotypes, energy expenditure varied linearly as functions of decreasing ambient temperature. However, a greater response (*i.e.* Δenergy expenditure/Δambient temperature) was observed in $Them2^{-/-}$ mice, and this was attributable to the effect of Them2 expression on energy expenditure in the light phase (Fig. 3*E*).

A separate experimental design explored the effects of Them2 expression nearer to steady state, by more prolonged equilibration and monitoring of mice at each of the three ambient temperatures. Fig. 4*A* shows the influence of Them2 expression on core body temperature in mice equilibrated at each ambient temperature for 48 h and then monitored for 48 h.

At 30 °C, *Them2*$^{-/-}$ mice exhibited similar core body temperatures to *Them2*$^{+/+}$ mice during the light phase. There were modest decreases in the core body temperatures of *Them2*$^{-/-}$ mice when compared with those of *Them2*$^{+/+}$ mice early during the first light phase at 22 °C, but this was diminished in the second. At 4 °C, diurnal variations in core body temperatures were largely lost, but core body temperatures were appreciably lower in *Them2*$^{-/-}$ mice. Under ambient temperature-equilibrated conditions, mean core body temperatures no longer decreased linearly as functions of temperature (Fig. 4*B*). Instead values in *Them2*$^{+/+}$ mice increased from 30 to 22 °C and then decreased at 4 °C, whereas values in *Them2*$^{-/-}$ mice decreased modestly from 30 to 22 °C and more steeply at 4 °C. When compared with *Them2*$^{+/+}$ mice, mean core body temperatures were decreased in *Them2*$^{-/-}$ mice during the light phase at 22 °C and throughout the diurnal cycle at 4 °C. Food consumption was increased in *Them2*$^{-/-}$ mice at 30 °C, due mainly to increases during the light phase (Fig. 4*C*). Although food intake was linear as a function of decreasing ambient temperature under these experimental conditions, there were no significant differences in the response of food intake due to genotype in these temperature-equilibrated mice (Fig. 4*D*).

Fig. 5 shows the influence of Them2 expression on mouse physical activity following more prolonged equilibration at each ambient temperature. Genotype-dependent effects on total (Fig. 5*A*) and ambulatory (Fig. 5*B*) activity paralleled those observed under adaptive conditions (Fig. 2), but became less pronounced at 22 °C prior to disappearing at 4 °C. *Them2*$^{-/-}$ mice were again more active over 24 h and during the dark phase at 30 °C, as reflected by increased total (Fig. 5*C*) and ambulatory activity (Fig. 5*D*). There were also significant increases in ambulatory activity during the light phase in *Them2*$^{-/-}$ mice. As was observed for mean core body temperatures (Fig. 4*B*), values of total and ambulatory activity in *Them2*$^{+/+}$ mice increased from 30 to 22 °C and then decreased at 4 °C, whereas corresponding values in *Them2*$^{-/-}$ mice decreased at 22 °C and again at 4 °C, particularly during the dark phase. Body weights (g) of *Them2*$^{+/+}$ mice equilibrated at 30 °C were lower than *Them2*$^{-/-}$ mice (*Them2*$^{+/+}$, 22.6 ± 0.6; *Them2*$^{-/-}$, 25.4 ± 0.6), but no differences were observed at either 22 °C (*Them2*$^{+/+}$, 23.5 ± 0.6; *Them2*$^{-/-}$, 24.8 ± 0.5) or 4 °C (*Them2*$^{+/+}$, 23.4 ± 0.6; *Them2*$^{-/-}$, 23.3 ± 0.4).

Fig. 6 demonstrates the influence of Them2 expression on gas exchange under ambient temperature-equilibrated conditions. At 30 °C, VO_2 values were again increased for both genotypes at the beginning of the dark phase, with greater increases in *Them2*$^{-/-}$ mice (Fig. 6*A*). However, these differences were no longer apparent as the ambient temperature was decreased. RER values were modestly increased in *Them2*$^{-/-}$ mice at 30 °C during both the light and the dark phases (Fig. 6*B*). At 22 °C, values of RER were higher in *Them2*$^{+/+}$ mice only during the light phases. Exposure to an ambient temperature of 4 °C again resulted in a decline in RER values, but there was no appreciable difference attributable to genotype. Rates of energy expenditure (Fig. 6*C*) mirrored VO_2 values (Fig. 6*A*), but there were no differences in cumulative energy expenditure apart from a non-significant increase in *Them2*$^{-/-}$ mice over 24 h at 30 °C (Fig. 6*D*). Under ambient temperature-equilibrated conditions, energy expenditure again varied linearly as functions of decreasing ambient temperature in both genotypes. However, there were no longer any differences in response based upon genotype (Fig. 6*E*).

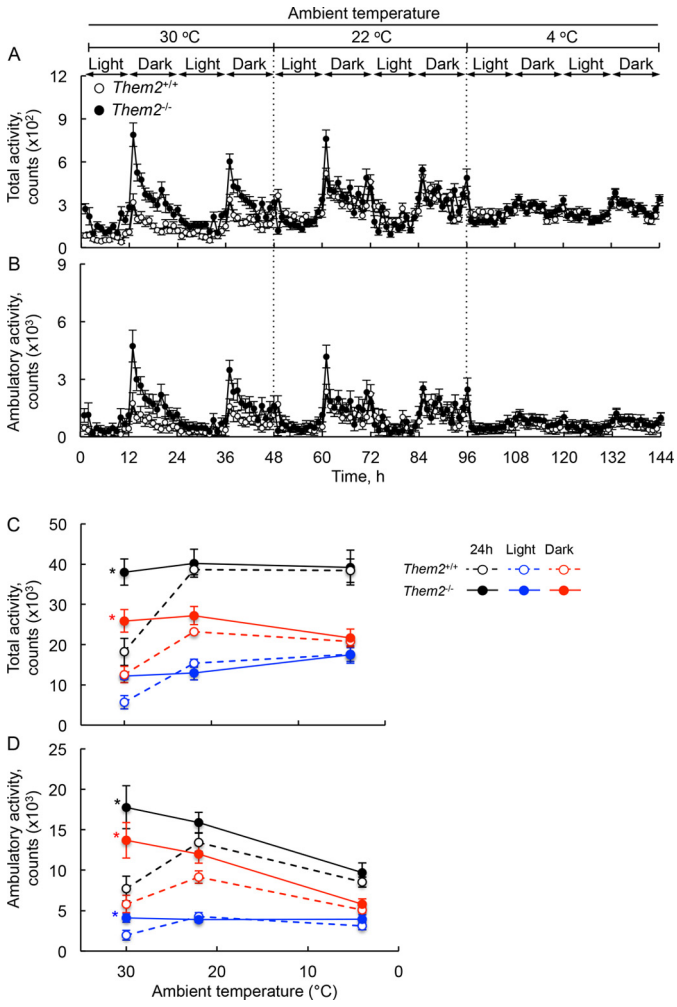

FIGURE 5. **Influence of Them2 expression on physical activity of ambient temperature-equilibrated mice.** *A* and *B*, total (*A*) and ambulatory (*B*) activities were monitored in the CLAMS experiment described in the legend for Fig. 4. *Vertical dashed lines* denote intervening 48-h equilibration periods. *C* and *D*, total (*C*) and ambulatory (*D*) activities were determined for the 48-h period, as well as the two 12-h light and dark phases indicated in *panel A*. Values were divided by 2 to facilitate comparisons with the respective adaptive responses (Fig. 2, *C* and *D*) over a 24-h period. *, $p < 0.05$, *Them2*$^{+/+}$ *versus* *Them2*$^{-/-}$.

Influence of Food and Light Exposure on Core Body Temperature and Energy Expenditure—We next investigated whether the genotype-dependent effects observed at 22 °C during the beginning of dark phase was influenced by food availability (Fig. 7, *A–E*) or light exposure (Fig. 7, *F–J*). Although the smaller numbers of mice ($n = 3$/group) used in these experiments were associated with more data dispersion when compared with those in Figs. 1–6, they nevertheless permitted the detection of substantial changes. When food was removed at the beginning of the dark phase, both genotypes still exhibited increased core body temperatures at the inception of the dark phase, with higher temperatures observed for *Them2*$^{-/-}$ mice (Fig. 7*A*). Refeeding during the light phase led to a brisk increase in body temperature for both genotypes, but this increase was again

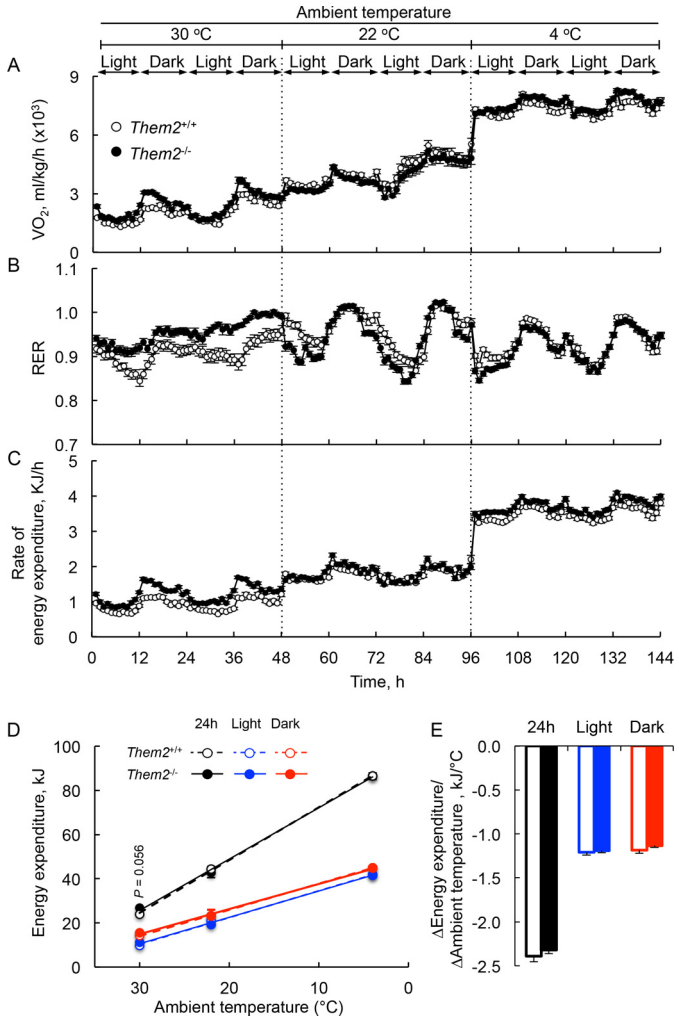

FIGURE 6. **Influence of Them2 expression on energy expenditure of ambient temperature-equilibrated mice.** *A–C*, VO_2 (*A*) and RER (*B*) were monitored in the CLAMS experiment described in the legend for Fig. 4 and used to calculate rates of energy expenditure (*C*). *Vertical dashed lines* denote intervening 48-h equilibration periods. *D*, values of energy expenditure for the 48-h period, as well as the two 12-h light and dark phases indicated in *panel A*, were adjusted for lean body weight and compared by analysis of covariance as described under "Experimental Procedures." Values were divided by 2 to facilitate comparisons with the respective adaptive responses (Fig. 3, *C* and *D*) over a 24-h period. *E*, responses of energy expenditure to changes in ambient temperature (ΔEnergy expenditure/ΔAmbient temperature) were determined by calculating slopes of linear regression lines for individual mice in *panel C*. *, $p < 0.05$, $Them2^{+/+}$ *versus* $Them2^{-/-}$.

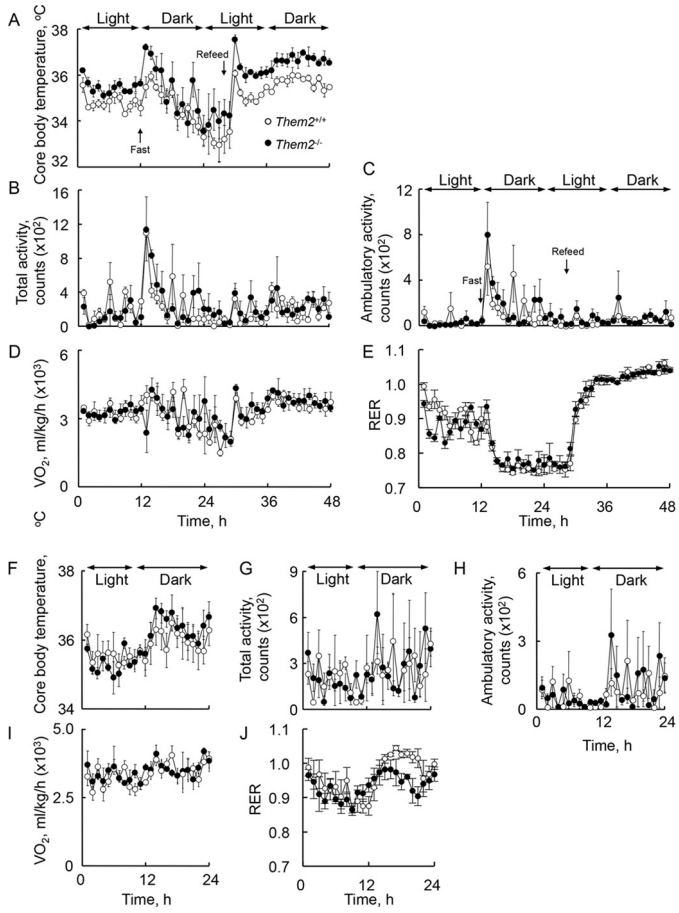

FIGURE 7. **Influence of feeding and light cycle on body temperature, physical activity and gas exchange.** Mice were subjected to CLAMS at 22 °C over a 24-h period. *A–E*, as indicated by the *arrows*, food access was restricted (*Fast*) at the beginning time of a dark cycle and then reintroduced (*Refeed*) following a 16-h fast (n = 3/group). *F–J*, the same mice were allowed to recover for 1 week and then subjected to a variation in light/dark cycle schedule in which the dark cycle was shifted to 2 h earlier. *A* and *F*, core body temperature; *B* and *G*, total activity; *C* and *H*, ambulatory activity; *D* and *I*, VO_2; *E* and *J*, RER.

higher in $Them2^{-/-}$ mice. After reaching a peak and declining, the difference in core body temperature persisted for the remainder of the experiment. Similarly, food withdrawal did not abrogate the increase in total (Fig. 7*B*) or ambulatory (Fig. 7*C*) activity observed at the beginning of the dark phase. However, the magnitude of the increase was similar in both $Them2^{+/+}$ and $Them2^{-/-}$ mice under these conditions. Refeeding did not influence physical activity for either genotype, but there was no longer a spike in physical activity at the transition to the next dark phase. Food withdrawal eliminated the increases in VO_2 values, as well as the difference observed between genotypes (Fig. 7*D*), and produced an expected decline in RER values (Fig. 7*E*). Refeeding led to rapid increases in both values and tended to restore the higher values previously observed for $Them2^{-/-}$ mice.

When the beginning of the dark phase was shifted to 2 h ahead of the regular schedule, the time at which core body temperature increased did not change for either genotype (Fig. 7*F*), although the magnitude of the increase appeared somewhat attenuated for $Them2^{-/-}$ mice. Similarly, the pattern of physical activity was largely unchanged by the acute change in light exposure (Fig. 7, *G* and *H*). By contrast, there were no apparent increases in VO_2 values in response to earlier exposure of mice to the dark (Fig. 7*I*), although values or RER began to rise in both genotypes (Fig. 7*J*).

Influence of Them2 Expression on Structure and Function of BAT—To gain further insights into Them2-mediated regulation of energy homeostasis, we examined the influence of Them2 expression on BAT. As assessed by microCT, total BAT was reduced by 50% in $Them2^{-/-}$ mice (Fig. 8*A*). However, mitochondrial DNA contents and citrate synthase activities were unchanged (Fig. 8*B*). A histopathologic analysis of BAT revealed a decrease in lipid droplet size in the absence of Them2 expression (Fig. 8*C*). We also observed ultrastructural changes by electron microscopy; BAT cells from $Them2^{+/+}$ mice contained discrete mitochondria that were clearly demarcated

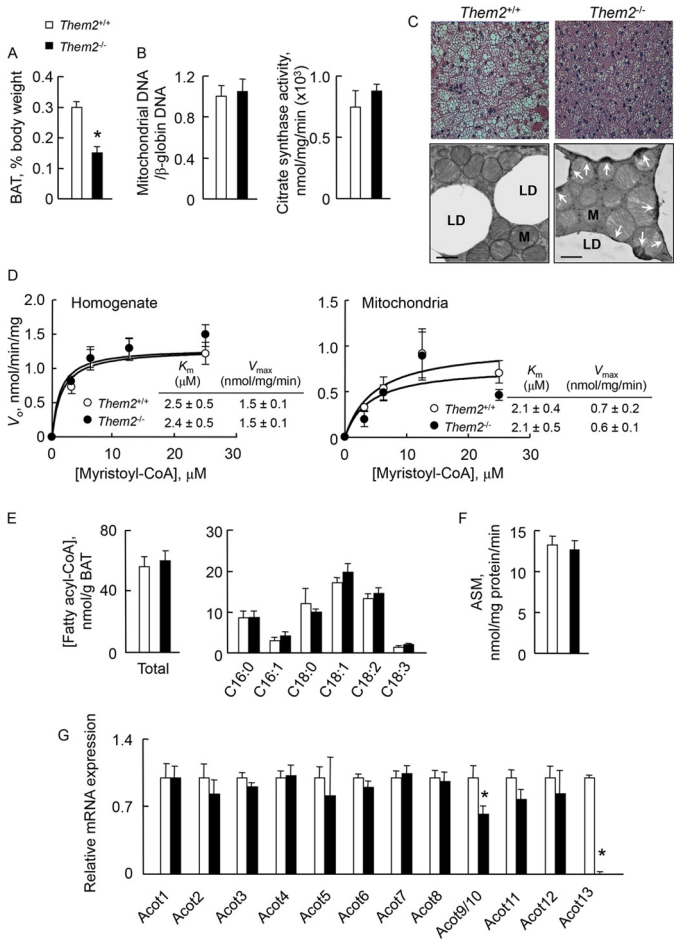

FIGURE 8. **Influence of Them2 expression on BAT.** *A*, the percentage of BAT was quantified by microCT. *B*, mitochondrial contents of BAT quantified according to DNA content and citrate synthase activity. *C*, BAT structure was assessed by hematoxylin and eosin staining (*top panels*) and electron microscopy (*bottom panels*). Abbreviations: *LD*, lipid droplet; *M*, mitochondria. The *bar* in each panel denotes 1 μm. *Arrows* denote areas of increased electron density in between lipid droplets and mitochondria in *Them2*$^{-/-}$ mice. *D*, acyl-CoA thioesterase activities in BAT were determined using homogenates ($n = 3$/group) and purified mitochondria (*Them2*$^{+/+}$, $n = 4$; *Them2*$^{-/-}$, $n = 5$). *E*, tissue concentrations of total fatty acyl-CoAs and individual fatty acyl-CoA molecular species were quantified in BAT of mice housed at room temperature ($n = 3$/group). *F*, fatty acid oxidation rates quantified according to acid-soluble metabolites (*ASM*) as described under "Experimental Procedures." *G*, mRNA expression of Acot genes in BAT ($n = 5$/group). In each experiment, mice were housed at room temperature. *, $p < 0.05$, *Them2*$^{+/+}$ *versus* *Them2*$^{-/-}$.

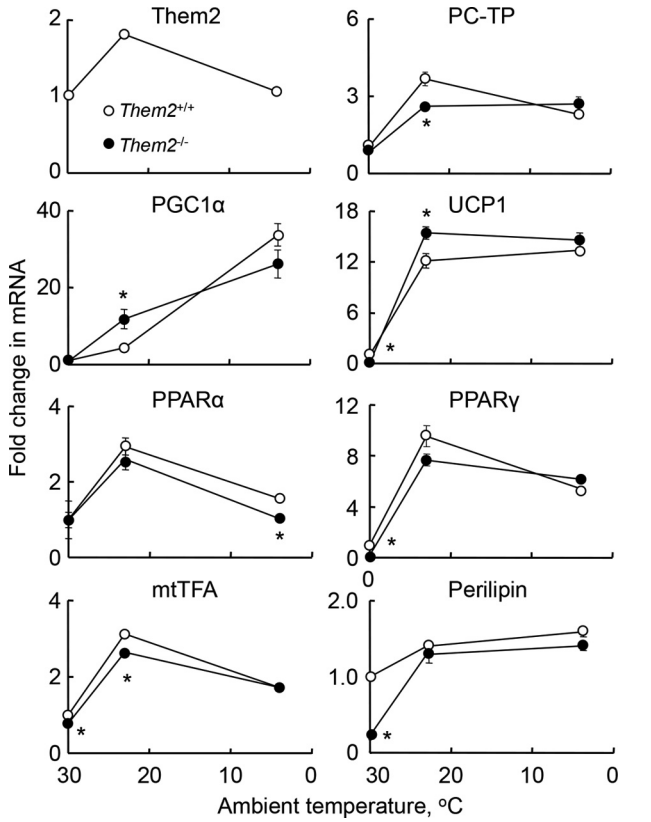

FIGURE 9. **Influence of Them2 expression on thermogenic gene expression in BAT.** mRNA expression of selected genes was determined in BAT harvested from mice housed for 24 h each at the indicated ambient temperatures. Expression levels were normalized to values in BAT of *Them2*$^{+/+}$ mice at 30 °C. *, $p < 0.05$, *Them2*$^{+/+}$ *versus* *Them2*$^{-/-}$.

from adjacent lipid droplets (Fig. 8*C*). By contrast in BAT from *Them2*$^{-/-}$ mice, mitochondria that were adjacent to lipid droplets exhibited electron-dense interfaces between the mitochondrion and the adjacent lipid droplet (Fig. 8*C*, *arrows*). Loss of Them2 expression did not alter fatty acyl-CoA thioesterase activity in BAT homogenates or isolated mitochondria (Fig. 8*D*). In keeping with this observation, total and individual fatty acyl-CoAs concentrations were not different in BAT from *Them2*$^{+/+}$ and *Them2*$^{-/-}$ mice (Fig. 8*E*). Rates of fatty acid oxidation in BAT homogenates were also unchanged (Fig. 8*F*). To assess whether the absence of Them2 expression might lead to compensatory increases in expression of another Acot, we compared mRNA levels of the other mammalian Acot genes. Apart from a 38% reduction in *Acot9/10* expression, there was no effect of *Them2* expression on *Acots* in BAT (Fig. 8*G*).

To gain additional insights into metabolic changes observed in response to changes in ambient temperature, BAT was harvested following 24 h of exposure to each temperature for measurements of mRNA expression levels for selected genes that participate in thermogenesis (Fig. 9). At 30 °C, mRNAs for *UCP1*, *PPARγ*, *mtTFA* (mitochondrial transcription factor A), and perilipin were decreased in BAT of *Them2*$^{-/-}$ relative to *Them2*$^{+/+}$ mice. At 22 °C, there was induction of expression for all of the genes in both genotypes. However, the absence of Them2 led to relatively higher mRNA levels of *PGC1α* and *UCP1* and to relatively lower levels of *PC-TP* and *mtTFA*. When the ambient temperature was decreased to 4 °C, mRNA expression levels tended to level off or decrease for all genes except *PGC1α*.

Increased Norepinephrine Sensitivity and Thermogenic Gene Expression in Them2$^{-/-}$ *Brown Adipocytes*—We utilized primary cultured brown adipocytes to examine evidence for a role of Them2 cellular norepinephrine-mediated lipolysis and fatty acid oxidation. Primary brown preadipocytes from *Them2*$^{-/-}$ were readily cultured and differentiated, exhibiting normal lipid droplet formation (data not shown). Indicative of higher rates of lipolysis, norepinephrine-stimulated increases in glycerol concentrations in culture media increased more rapidly in *Them2*$^{-/-}$ when compared with *Them2*$^{+/+}$ brown adipocytes (Fig. 10*A*). Although Them2 expression did not influence basal values of OCR, after remaining unchanged for ~30 min follow-

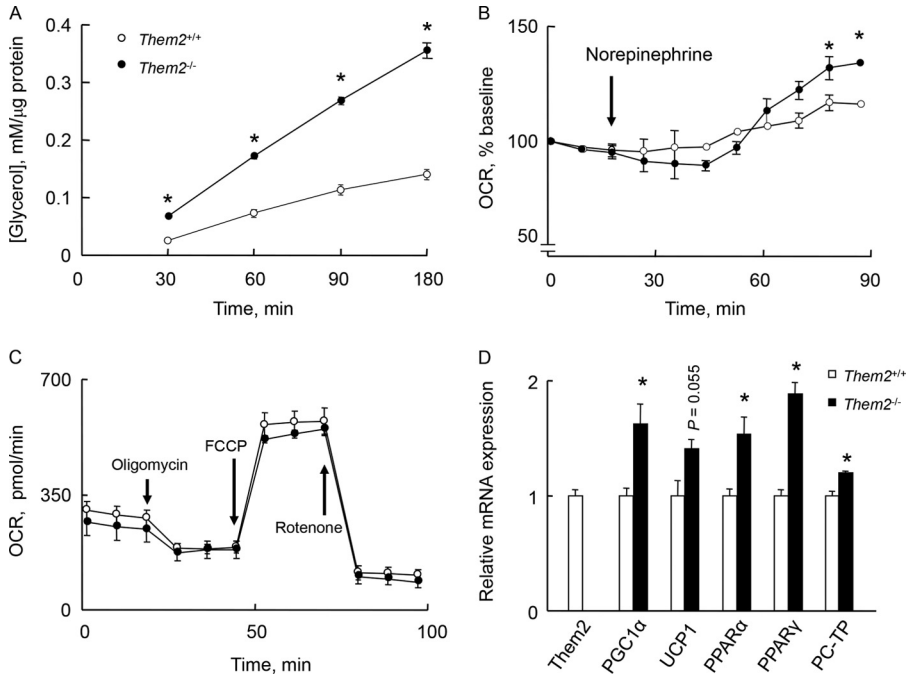

FIGURE 10. **Increased norepinephrine responsiveness in Them2-deficient primary brown adipocytes.** Primary brown preadipocytes isolated from BAT of mice housed at room temperature were cultured and then differentiated into mature brown adipocytes. *A*, lipolysis was determined by measuring glycerol concentrations ($n = 3$/group) from culture media following the addition of norepinephrine (1 μM). *B*, O_2 consumption rates (*OCR*) values were determined during an initial equilibration period and following norepinephrine (1 μM) addition to the media, as indicated by the *arrow*. *C*, OCR values were measured in primary brown adipocytes following the addition of ATP synthase inhibitor, oligomycin (1 μM), mitochondrial uncoupler, FCCP (0.5 μM), and electron transfer inhibitor, rotenone (1 μM), as indicated by the *arrows*. Because protein and mitochondrial DNA contents were identical in cultures of brown adipocytes from *Them2*$^{-/-}$ and *Them2*$^{+/+}$ mice (data not shown), OCR are represented as pmol/min. *D*, mRNA expression of selected genes was measured in differentiated primary brown adipocytes ($n = 3$/group). *, $p < 0.05$, *Them2*$^{+/+}$ *versus Them2*$^{-/-}$.

ing the addition of norepinephrine, OCR values increased more rapidly in *Them2*$^{-/-}$ brown adipocytes (Fig. 10*B*).

To further examine the impact of Them2 expression on cellular mitochondrial function, primary brown adipocytes were sequentially exposed to oligomycin, FCCP, and rotenone, which assess ATP-linked O_2 consumption, maximum OCR, and non-mitochondrial OCR, respectively (18). There were no differences in basal OCR values due to Them2 loss of expression, nor were there any other apparent changes in cellular bioenergetic parameters (Fig. 10*C*). Mature brown adipocytes lacking Them2 expression exhibited increases in mRNA levels of *PGC1α*, *PPARα*, and *PPARγ* and a trend toward increased *UCP1* (Fig. 10*D*). The absence of Them2 also led to an increase in *PC-TP* mRNA levels.

DISCUSSION

This study was designed to investigate the contribution of Them2 to the regulation of thermogenesis. Consistent with a role for Them2 in suppressing heat production in response to thermal stress, *Them2*$^{-/-}$ mice exhibited increased measures of adaptive energy expenditure that were most pronounced just following the transition from the light to dark phases of the diurnal cycle in mice housed at thermoneutrality (30 °C) (6) and at room temperature (22 °C), whereas in the cold (4 °C), this increase was persistent throughout the diurnal cycle. With the exception of modest increases at thermoneutrality, mice equilibrated for longer periods did not exhibit genotype-dependent differences in measures of energy expenditure. This suggests that Them2 does not play a central role in regulating steady state energy expenditure or that compensatory mechanisms are engaged that largely negate its effects.

In our initial study describing *Them2*$^{-/-}$ mice, we observed reductions in body weight when compared with *Them2*$^{+/+}$ mice despite increased rates of food consumption (11). Based on our inability to appreciate significant increases in energy expenditure under these experimental conditions, we attributed the findings primarily to a modest decrease in intestinal lipid absorption (11). Considering that the prior experiments were conducted essentially at the steady state ambient room temperature of 22 °C, we failed to appreciate the potential contribution of increased adaptive thermogenesis in *Them2*$^{-/-}$ mice that was revealed in the current study. Presumably, mice housed under standard conditions are subjected to intermittent thermal stress related to housing density and ambient temperature fluctuations (15, 19). The more robust response of adaptive energy expenditure to ambient temperature in the absence of Them2 expression likely contributed the reductions in body weight and adiposity observed in these mice over time.

Under adaptive conditions, the current analysis also demonstrated that increases in food consumption in *Them2*$^{+/+}$ mice were closely associated with several measures of higher energy expenditure (*i.e.* increased core body temperatures, physical activities, and cumulative energy expenditure). Greater food consumption in the absence of Them2 expression most likely occurred in response to the metabolic demands of increased energy expenditure (20) and suggests that the modest changes in intestinal lipid absorption observed previously (11) made

only minor contributions to differences in body weight. Appreciating the complex relationships between circadian and metabolic oscillations (21), we nevertheless attempted to discern whether Them2 expression might have influenced food intake or the amplitude of a circadian rhythm. Withholding of food tended to diminish differences in energy expenditure between *Them2*$^{-/-}$ and *Them2*$^{+/+}$ mice that occurred early in the dark phase. This implied that regulation of adaptive energy expenditure was a primary effect of Them2 expression, a function that was generally supported by experiments in which differences in core body temperature and activity between *Them2*$^{-/-}$ and *Them2*$^{+/+}$ mice fed *ad libitum* were preserved in the setting of varied light/dark cycles.

Considering that Them2 is robustly expressed in BAT (9), we explored evidence for a primary role for Them2 in regulating thermogenesis. The reduction in BAT quantified by microCT was most likely attributable to the reduced lipid droplet sizes, which had been observed histologically. When taken together with ultrastructural evidence consistent with increased mitochondrial fatty acid uptake, these findings were suggestive of increased BAT activity in *Them2*$^{-/-}$ mice. This possibility was in keeping with up-regulation of expression of the thermogenic genes *PGC1α* and *UCP1* at 22 °C, the ambient temperature at which the effect of Them2 expression was most pronounced. Presumably because glucose uptake and oxidation follow the activation of thermogenesis in BAT (22), we did not observe marked changes in RER values for *Them2*$^{-/-}$ mice.

Them2 exhibits Acot activity for long chain acyl-CoAs (9), and we have demonstrated reductions in Acot activity in liver homogenates and isolated mitochondria from livers of *Them2*$^{-/-}$ mice, along with increases in tissue concentrations of fatty acyl-CoAs (11) when compared with samples from *Them2*$^{+/+}$ mice. In BAT from *Them2*$^{-/-}$ mice, however, we were unable to detect a difference in enzymatic activity when compared with BAT from *Them2*$^{+/+}$ mice. This most likely reflects concurrent expression of other Acot genes, which would have been expected to contribute to the activity that we measured and presumably made it impossible to detect the selective absence of Them2. The presence of other Acots could explain the absence of increases in fatty acyl-CoA concentrations and rates of fatty acid oxidation in BAT homogenates from *Them2*$^{-/-}$ mice. It is also possible that the biochemical consequences of Them2 expression would only be detected in *ex vivo* assays of BAT if mice were sacrificed in the early hours of the dark phase, which was not the case in these studies.

More likely, the absence of increased rates of fatty acid oxidation in BAT tissue of *Them2*$^{-/-}$ mice *ex vivo* was because the use of homogenized tissue in the assay did not replicate the necessary cellular structures and architecture required to detect increased fatty acid channeling from lipid droplets to mitochondria *in vivo*. This possibility is supported by the electron-dense interfaces between mitochondria and smaller lipid droplets in BAT of *Them2*$^{-/-}$ mice, as well as by experiments in primary brown adipocytes, which suggest a direct role for Them2 in thermogenesis. Increased norepinephrine-stimulated glycerol release was consistent with enhanced rates of lipolysis. Although this occurred in the absence of an increase in expression of perilipin mRNA, perilipin-mediated control of lipolysis is regulated primarily by phosphorylation (23), which was not explored in our study. Although we did not observe increases in basal OCR values or differences in mitochondrial respiratory capacity, *Them2*$^{-/-}$ brown adipocytes did exhibit an increase in norepinephrine-stimulated OCR values. This response was in keeping with increased rates of lipolysis in the absence of Them2 expression. As observed in cells lacking Them1, thermogenic genes were induced in *Them2*$^{-/-}$ brown adipocytes. Future studies of the role of Them2 in the release of fatty acids from triglyceride droplets and their delivery to mitochondria should shed additional light on the molecular mechanism by which Them2 suppresses energy expenditure.

Although both *in vivo* and *in vitro* evidence suggest that Them2 expression in BAT was primarily responsible for alterations in energy homeostasis, *Them2*$^{-/-}$ mice were globally deficient in Them2. Because Them2 is also expressed in a variety of tissues, including the brain (24), which plays a critical role in regulating thermogenesis (25), we cannot exclude indirect contributions of Them2 to this regulation, such as CNS-mediated control. In this connection, a recent study using targeted deletion in neurons revealed that Acot7 accounts for most of the thioesterase activity in brain (26). Among the phenotypes attributable to loss of neuronal Acot7 were increased physical activity and energy expenditure during fasting and increased thermogenesis during cold exposure. These data were accompanied by evidence that a hyperactive neural response to physiological challenges was the mechanism, and that this was due to alterations in either the adrenergic input to BAT or the tissue response.

Although the detailed molecular mechanisms are not yet understood, observations in mice with disruption of *Them1* and *Them2* suggest that the dynamic interconversion of long chain fatty acyl-CoAs and free fatty acids within BAT plays an important role in the regulation of adaptive thermogenesis. This would be in keeping with the demonstration that ACSL1, which catalyzes the conversion of free fatty acids to long acyl-CoAs, promotes fatty acid oxidation and energy expenditure in BAT (1). For *Them2*$^{-/-}$ mice, this occurred in the absence of intrinsic changes in mitochondrial function, suggesting that metabolic control is due at least in part to the control of fatty acid channeling.

Acknowledgments—The use of the Longwood Small Animal Imaging Facility at Beth Israel Deaconess Medical Center (Boston, MA) was supported in part by National Institutes of Health/National Center for Research Resources shared instrumentation Grant S10-RR-023010. The use of the Rodent Histopathology Core Facility of Dana-Farber/Harvard Cancer Center (Boston, MA) was supported in part by an NCI Cancer Center Support Grant, National Institutes of Health Grant P30 CA06516. The use of the Mouse Metabolic Phenotype Center at Yale University School of Medicine (New Haven, CT) was supported in part by National Institutes of Health Grant U24 DK76169.

REFERENCES

1. Ellis, J. M., Li, L. O., Wu, P. C., Koves, T. R., Ilkayeva, O., Stevens, R. D., Watkins, S. M., Muoio, D. M., and Coleman, R. A. (2010) Adipose acyl-CoA synthetase-1 directs fatty acids toward -oxidation and is required for

cold thermogenesis. *Cell Metab.* **12,** 53–64
2. Brocker, C., Carpenter, C., Nebert, D. W., and Vasiliou, V. (2010) Evolutionary divergence and functions of the human acyl-CoA thioesterase gene (ACOT) family. *Hum. Genomics* **4,** 411–420
3. Kirkby, B., Roman, N., Kobe, B., Kellie, S., and Forwood, J. K. (2010) Functional and structural properties of mammalian acyl-coenzyme A thioesterases. *Prog. Lipid Res.* **49,** 366–377
4. Cohen, D. E. (2013) New players on the metabolic stage: How do you like Them Acots? *Adipocyte* **2,** 3–6
5. Zhang, Y., Li, Y., Niepel, M. W., Kawano, Y., Han, S., Liu, S., Marsili, A., Larsen, P. R., Lee, C. H., and Cohen, D. E. (2012) Targeted deletion of thioesterase superfamily member 1 promotes energy expenditure and protects against obesity and insulin resistance. *Proc. Natl. Acad. Sci. U.S.A.* **109,** 5417–5422
6. Cannon, B., and Nedergaard, J. (2004) Brown adipose tissue: function and physiological significance. *Physiol. Rev.* **84,** 277–359
7. Hunt, M. C., and Alexson, S. E. (2002) The role acyl-CoA thioesterases play in mediating intracellular lipid metabolism. *Prog. Lipid Res.* **41,** 99–130
8. Kanno, K., Wu, M. K., Agate, D. S., Fanelli, B. J., Wagle, N., Scapa, E. F., Ukomadu, C., and Cohen, D. E. (2007) Interacting proteins dictate function of the minimal START domain phosphatidylcholine transfer protein/StarD2. *J. Biol. Chem.* **282,** 30728–30736
9. Wei, J., Kang, H. W., and Cohen, D. E. (2009) Thioesterase superfamily member 2 (Them2)/acyl-CoA thioesterase 13 (Acot13): A homotetrameric hotdog fold thioesterase with selectivity for long-chain fatty acyl-CoAs. *Biochem. J.* **421,** 311–322
10. Cao, J., Xu, H., Zhao, H., Gong, W., and Dunaway-Mariano, D. (2009) The mechanisms of human hotdog-fold thioesterase 2 (hTHEM2) substrate recognition and catalysis illuminated by a structure and function based analysis. *Biochemistry* **48,** 1293–1304
11. Kang, H. W., Niepel, M. W., Han, S., Kawano, Y., and Cohen, D. E. (2012) Thioesterase superfamily member 2/acyl-CoA thioesterase 13 (Them2/Acot13) regulates hepatic lipid and glucose metabolism. *FASEB J.* **26,** 2209–2221
12. McLean, J. A., and Tobin, G. (1987) *Animal and Human Calorimetry*, Cambridge University Press, Cambridge, UK
13. Arch, J. R., Hislop, D., Wang, S. J., and Speakman, J. R. (2006) Some mathematical and technical issues in the measurement and interpretation of open-circuit indirect calorimetry in small animals. *Int. J. Obes.* (*Lond.*) **30,** 1322–1331
14. Tschöp, M. H., Speakman, J. R., Arch, J. R., Auwerx, J., Brüning, J. C., Chan, L., Eckel, R. H., Farese, R. V., Jr., Galgani, J. E., Hambly, C., Herman, M. A., Horvath, T. L., Kahn, B. B., Kozma, S. C., Maratos-Flier, E., Müller, T. D., Münzberg, H., Pfluger, P. T., Plum, L., Reitman, M. L., Rahmouni, K., Shulman, G. I., Thomas, G., Kahn, C. R., and Ravussin, E. (2012) A guide to analysis of mouse energy metabolism. *Nat. Methods* **9,** 57–63
15. Kang, H. W., Ribich, S., Kim, B. W., Hagen, S. J., Bianco, A. C., and Cohen, D. E. (2009) Mice lacking phosphatidylcholine transfer protein/StarD2 exhibit increased adaptive thermogenesis and enlarged mitochondria in brown adipose tissue. *J. Lipid Res.* **50,** 2212–2221
16. Vernochet, C., Mourier, A., Bezy, O., Macotela, Y., Boucher, J., Rardin, M. J., An, D., Lee, K. Y., Ilkayeva, O. R., Zingaretti, C. M., Emanuelli, B., Smyth, G., Cinti, S., Newgard, C. B., Gibson, B. W., Larsson, N. G., and Kahn, C. R. (2012) Adipose-specific deletion of TFAM increases mitochondrial oxidation and protects mice against obesity and insulin resistance. *Cell Metab.* **16,** 765–776
17. Souza, S. C., Muliro, K. V., Liscum, L., Lien, P., Yamamoto, M. T., Schaffer, J. E., Dallal, G. E., Wang, X., Kraemer, F. B., Obin, M., and Greenberg, A. S. (2002) Modulation of hormone-sensitive lipase and protein kinase A-mediated lipolysis by perilipin A in an adenoviral reconstituted system. *J. Biol. Chem.* **277,** 8267–8272
18. Hill, B. G., Benavides, G. A., Lancaster, J. R., Jr., Ballinger, S., Dell'Italia, L., Zhang, J., and Darley-Usmar, V. M. (2012) Integration of cellular bioenergetics with mitochondrial quality control and autophagy. *Biol. Chem.* **393,** 1485–1512
19. Nagy, T. R., Krzywanski, D., Li, J., Meleth, S., and Desmond, R. (2002) Effect of group *vs.* single housing on phenotypic variance in C57BL/6J mice. *Obes. Res.* **10,** 412–415
20. Kozak, L. P. (2010) Brown fat and the myth of diet-induced thermogenesis. *Cell Metab.* **11,** 263–267
21. Asher, G., and Schibler, U. (2011) Crosstalk between components of circadian and metabolic cycles in mammals. *Cell Metab.* **13,** 125–137
22. Cannon, B., and Nedergaard, J. (2010) Metabolic consequences of the presence or absence of the thermogenic capacity of brown adipose tissue in mice (and probably in humans). *Int. J. Obes.* (*Lond.*) **34,** S7–S16
23. Souza, S. C., Christoffolete, M. A., Ribeiro, M. O., Miyoshi, H., Strissel, K. J., Stancheva, Z. S., Rogers, N. H., D'Eon, T. M., Perfield, J. W., 2nd, Imachi, H., Obin, M. S., Bianco, A. C., and Greenberg, A. S. (2007) Perilipin regulates the thermogenic actions of norepinephrine in brown adipose tissue. *J. Lipid Res.* **48,** 1273–1279
24. Cheng, Z., Bao, S., Shan, X., Xu, H., and Gong, W. (2006) Human thioesterase superfamily member 2 (hTHEM2) is co-localized with β-tubulin onto the microtubule. *Biochem. Biophys. Res. Commun.* **350,** 850–853
25. Clapham, J. C. (2012) Central control of thermogenesis. *Neuropharmacology* **63,** 111–123
26. Ellis, J. M., Wong, G. W., and Wolfgang, M. J. (2013) Acyl coenzyme a thioesterase 7 regulates neuronal fatty acid metabolism to prevent neurotoxicity. *Mol. Cell Biol.* **33,** 1869–1882